An open problem in pattern forming systems

Edward McDugald

November 27, 2022

1   Introduction

The aim of this report is to describe an open problem in pattern forming systems, pertaining specifically to patterns deriving from microscopic gradient flows that are translationally and rotationally invariant, and that admit straight parallel roll solutions on infinite domains. On finite domains however, such rolls may emerge in different locations with different orientations, and they meet in the interior of the domain generating point and line defects. Such pattern forming systems, while arising from various microscopic gradient systems, obey a universal PDE describing the evolution of the phase variable, θ.

A canonical example of such patterns in nature is seen through Rayleigh-Bénard convection. Rayleigh-Bénard convection may be observed by trapping a thin layer of fluid between two plates, and applying heat to the bottom plate. In the microscopic model which we will consider, the stress parameter R is the difference in heat between the top and bottom plate. Initially heat will transfer through the fluid by conduction, however past a critical value, heat will transfer through convection, generating a velocity field that manifests as temperature rolls in the fluid. In the figures we will present in this report, we may consider the surfaces as being the average temperature along the z direction.

The procedure for deriving such a phase equation involves studying the vector field whose components are the instantaneous frequencies of the pattern generated by the microscopic equations. We call this vector field $\boldsymbol{k}$, and note that this is the gradient of the phase, $\boldsymbol{k} = \nabla\theta$. The phase gradient is modulated over distances L, the average distance between defects, which is long with respect to the local wavelength l. We introduce the following
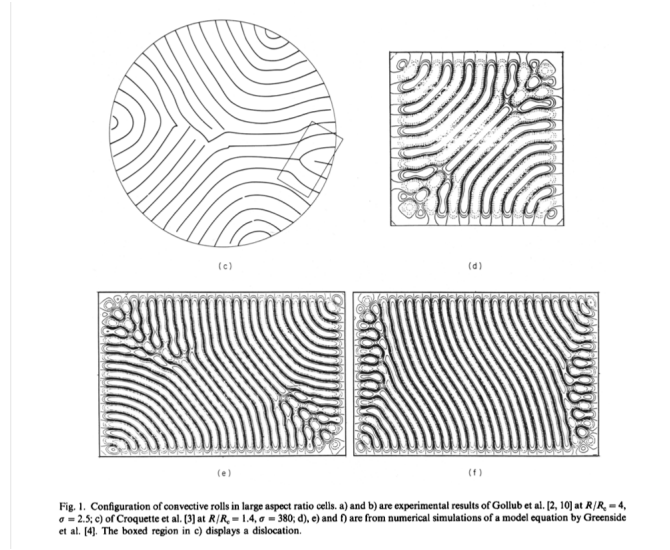
1

Fig. 1. Configuration of convective rolls in large aspect ratio cells. a) and b) are experimental results of Gollub et al. [2, 10] at $R/R_c = 4$, $\sigma = 2.5$; c) of Croquette et al. [3] at $R/R_c = 1.4$, $\sigma = 380$; d), e) and f) are from numerical simulations of a model equation by Greenside et al. [4]. The boxed region in c) displays a dislocation.

Figure 1.1: Numerical and experimental depictions of convection rolls.

Steady Convection Rolls: contours of temperature and the vector velocity field for a two-dimensional domain heated from below at Ra = 1800
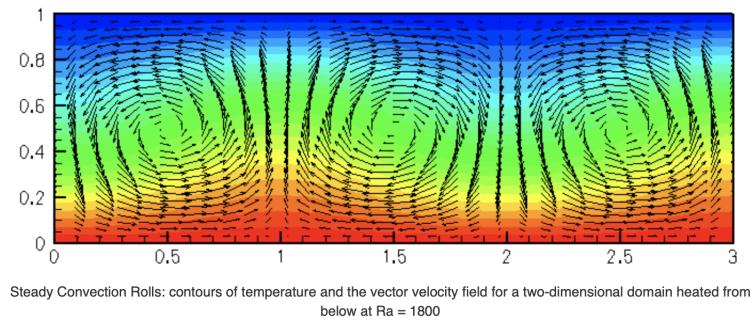
Figure 1.2: Local Periodicity of convection rolls.

variables:

$$X = \epsilon x$$
$$T = \epsilon^2 t$$
$$\Theta(X, T) = \epsilon \theta(x, t)$$
$$k = \|\boldsymbol{k}\|$$
$$\epsilon = \frac{l}{L} \quad \text{The inverse aspect ratio.}$$

Letting w be the variable of the microscopic equations, and E the associated energy functional, we apply the following modulational Ansatz:

$$w = \sum A_n(k^2)\cos(n\theta) \quad \text{(for real fields)} \tag{1.1}$$

$$w = A(k^2, X, T)e^{i\theta(x,t)} \quad \text{(for complex fields).} \tag{1.2}$$

We then average the energy over the peridicity of the pattern

$$\overline{E} = \frac{1}{2\pi}\int E d\theta \tag{1.3}$$

and analyze the dependence of the energy on A and Θ in orders of ϵ^n. We find that the only orders of ϵ that contribute are $\mathcal{O}(\epsilon^0)$ and $\mathcal{O}(\epsilon^2)$, and that the energy can be interpreted as a sum of stretching and bending energies. We also find that stationary solutions can be deduced by balancing the stress and strain energies. We pose an open challenge, where a certain pattern appearing in simulations of microscopic gradient flows, and in experiments, is not yet deduced by the Cross-Newell equation. We also discuss some potential uses of machine learning to approach this problem.

2 The Regularized Cross-Newell Phase Diffusion Equation for Complex Fields

2.1 Deriving the Unegularized Equation

We consider pattern forming systems that arise as PDEs that are equivalently gradient flows. These are a very general object, and we take as our preferred example to be the Swift Hohenberg equation. In its complexified form, the swift hohenberg equation has energy density

$$E = \int \left((\nabla^2 + 1)w(\nabla^2 + 1)w^* - Rww^* + \frac{1}{2}w^2w^{*2} \right) dx. \tag{2.1}$$

Let us compute δE,

$$\delta E = \lim_{h \to 0} \frac{E[w + h\delta w, w^* + h\delta w^*] - E[w, w^*]}{h}$$

$$= \int \Big((\nabla^2 + 1)w(\nabla^2 + 1)\delta w^* - Rw\delta w^* + w^2 w^* \delta w^* +$$

$$(\nabla^2 + 1)\delta w(\nabla^2 + 1)w^* - Rw^*\delta w + ww^{*2}\delta w \Big) d\boldsymbol{x}$$

Using integration by parts, one finds that

$$(\nabla^2 + 1)w(\nabla^2 + 1)\delta w^* = (\nabla^2 + 1)^2 w\delta w^*$$
$$(\nabla^2 + 1)\delta w(\nabla^2 + 1)^2 w^* = (\nabla^2 + 1)^2 w^* \delta w.$$

Thus, one obtains

$$\frac{\delta E}{\delta w^*} = (\nabla^2 + 1)^2 w - Rw + w^2 w^* \tag{2.2}$$

$$\frac{\delta E}{\delta w} = (\nabla^2 + 1)^2 w^* - Rw^* + w^{*2} w. \tag{2.3}$$

The complexified Swift-Hohenberg equations can be written as

$$w_t = -\frac{\delta E}{\delta w^*}, \quad w_2^* = -\frac{\delta E}{\delta w}. \tag{2.4}$$

Using the Ansatz for complex fields (1.2), one can write

$$\delta E = \frac{\delta E}{\delta w}\delta w + \frac{\delta E}{\delta w^*}\delta w^* = -2A_t \delta A - 2A^2\Theta_t \delta\theta. \tag{2.5}$$

We want now to find expressions for $\frac{\delta E}{\delta A}$ and $\frac{\delta E}{\delta \Theta}$ Using the fact that $\nabla_{\boldsymbol{x}} = \epsilon \nabla_{\boldsymbol{X}}$, and writing $w = Ae^{i\theta} = A(\boldsymbol{x})e^{i\theta(\boldsymbol{x})}$, one obtains

$$\nabla_{\boldsymbol{x}} w = e^{i\theta}(i\boldsymbol{k} + \epsilon \nabla_{\boldsymbol{X}})A \tag{2.6}$$

$$\nabla_{\boldsymbol{x}}^2 w = e^{i\theta}(-k^2 + i\epsilon(2\boldsymbol{x} \cdot \nabla_{\boldsymbol{X}} + \nabla_{\boldsymbol{X}} \cdot \boldsymbol{k}) + \epsilon^2 \nabla_{\boldsymbol{X}}^2)A \tag{2.7}$$

$$\nabla_{\boldsymbol{x}} w^* = e^{-i\theta}(-i\boldsymbol{k} + \epsilon \nabla_{\boldsymbol{X}})A \tag{2.8}$$

$$\nabla_{\boldsymbol{x}}^2 w^* = e^{-i\theta}(-k^2 - i\epsilon(2\boldsymbol{x} \cdot \nabla_{\boldsymbol{X}} + \nabla_{\boldsymbol{X}} \cdot \boldsymbol{k}) + \epsilon^2 \nabla_{\boldsymbol{X}}^2)A. \tag{2.9}$$

Inserting (1.2) into (2.1) with (2.6)-(2.9), and *ignoring* terms of order $\mathcal{O}(\epsilon^3)$, one obtains

$$E = \int \left((k^2 - 1)^2 A^2 - RA^2 + \frac{1}{4}A^4 + K \right) d\boldsymbol{x} \tag{2.10}$$

$$+ \epsilon^2 \int \left((2\boldsymbol{k} \cdot \nabla A + \nabla \cdot \boldsymbol{k}A)^2 + 2(1 - k^2)A\nabla^2 A \right) d\boldsymbol{x}.$$

Now, obtaining macroscopic equations in terms of the phase parameter requires averaging the energy over the periodicity of the pattern. Conveniently, in the complex field case, this averaging occurs automatically, and we have $E = \overline{E}$. Equation (2.5) gives

$$-2A_t = \frac{\delta \overline{E}}{\delta A} = \frac{\delta \overline{E_0}}{\delta A} + \epsilon^2 \frac{\delta \overline{E_2}}{\delta A}. \tag{2.11}$$

By construction, $A_t = \epsilon^2 A_T$, and therefore A_t is at most $\mathcal{O}(\epsilon^2)$. Thus, to leading order, the main equation contributing to the evolution of the amplitude A is

$$\frac{\delta \overline{E_0}}{\delta A} = 0. \tag{2.12}$$

This gives

$$A^2 = R - (K^2 - 1)^2. \tag{2.13}$$

This is known as the eikonal solution, which demands that the amplitude be slaved algebraically to the modulus of the phase gradient. This property holds for stress parameter values far from onset.

Having found a dominant relation for A, we seek an equation for Θ. Using the eikonal solution, we can write the leading order energy as

$$\overline{E_0} = \int -\frac{1}{2} \left(A^2(k^2) \right)^2 + K. \tag{2.14}$$

Considering just the $\mathcal{O}(\epsilon^0)$ contribution, equation (2.5) gives

$$A^2 \theta_t = -\frac{1}{2} \frac{\delta \overline{E_0}}{\delta \theta}. \tag{2.15}$$

We have

$$\frac{\delta \overline{E_0}}{\delta \theta} \delta \theta = \delta \left(-\frac{1}{2} (A^2(k^2))^2 \right)$$

$$= -A^2(k^2) \frac{d}{dk^2} A^2(k^2) 2\boldsymbol{k} \cdot \delta \nabla \theta.$$

Using integration by parts, one finds that

$$-A^2(k^2) \frac{d}{dk^2} A^2(k^2) 2\boldsymbol{k} \cdot \delta \nabla \theta = A^2(k^2) \frac{d}{dk^2} A^2(k^2) 2\nabla \cdot \boldsymbol{k} \delta \theta.$$

Thus, we obtain

$$A^2 \theta_t = -A^2(k^2) \frac{dA^2(k^2)}{dk^2} 2\nabla \cdot \boldsymbol{k}$$

Noting that $\theta_t = \epsilon \Theta_t$, $\nabla_{\boldsymbol{x}} = \epsilon \nabla_{\boldsymbol{X}}$, and setting

$$B(k^2) = A^2(k^2) \frac{dA^2(k^2)}{dk^2}, \tag{2.16}$$

one obtains the *unregularized* Cross-Newell phase diffusion equation

$$A^2 \Theta_T + \nabla_{\boldsymbol{X}} \cdot \boldsymbol{k} B(k^2) = 0. \tag{2.17}$$

5

2.2 Regularizing the Cross-Newell phase diffusion equation

Recall the form of $\overline{E_0}$, $\overline{E_0} = \int -\frac{1}{2}A^4(k^2) + K$. Let us define k_B to be the preferred wave number, by which we mean the wave number that minimizes E_0. That is, k_B is defined to satisfy the equation

$$\frac{d}{dk^2}A^4(k^2) = 0. \tag{2.18}$$

We define K to be $-\frac{1}{2}A^4(k^2)$ evaluated at k_B, and we can then write

$$\overline{E_0} = \int \left(-\frac{1}{2}A^4(k^2)\right)_{k^2}^{k_B^2} d\boldsymbol{x} \tag{2.19}$$

Note that this choice of K ensures that the leading order energy is 0 whenever $k = k_B$.

Let us look at the unregularized equation (2.17). We can write this as a diffusion equation in standard form

$$A^2\Theta_T = -\nabla_{\boldsymbol{X}}\left[B(k^2)\nabla\theta\right]. \tag{2.20}$$

Expanding the right hand side yields

$$A^2\Theta_T = \theta_{xx}\left(-\frac{dB(k^2)}{dk^2}2\theta_x^2 - B(k^2)\right) + \theta_{xy}\left(-\frac{dB(k^2)}{dk^2}4\theta_x\theta_y\right) + \theta_{yy}\left(-\frac{dB(k^2)}{dk^2}2\theta_y^2 - B(k^2)\right). \tag{2.21}$$

Consider the simple case where $\boldsymbol{k} = \langle\theta_x, 0\rangle$. We then obtain

$$A^2\Theta_T = \theta_{xx}\left(-\frac{dB(k^2)}{dk^2}2\theta_x^2 - B(k^2)\right) + \theta_{yy}\left(-B(k^2)\right).$$

To have a well-posed diffusion equation, we need that

$$-\frac{dB(k^2)}{dk^2}2\theta_x^2 - B(k^2) > 0 \tag{2.22}$$

$$-B(k^2) > 0 \tag{2.23}$$

Noting that

$$\frac{d}{dk}\left(kB(k^2)\right) = B(k^2) + k\frac{d}{dk}B(k^2) = B(k^2) + 2k^2\frac{d}{dk^2}B(k^2), \tag{2.24}$$

We see that we require

$$\frac{d}{dk}(kB(k^2)) < 0 \tag{2.25}$$

$$B(k^2) < 0. \tag{2.26}$$

It turns out that $B, (kB)'$ are the eigenvalues of the second order quasi-linear operator, and for all k the above must hold. Let us consider the plot of k vs kB. For the case of Swift-Hohenberg with $R = .5$, we have $B = -4(k^2 - 1)(.5 - (k^2 - 1)^2)$. We see that there is a
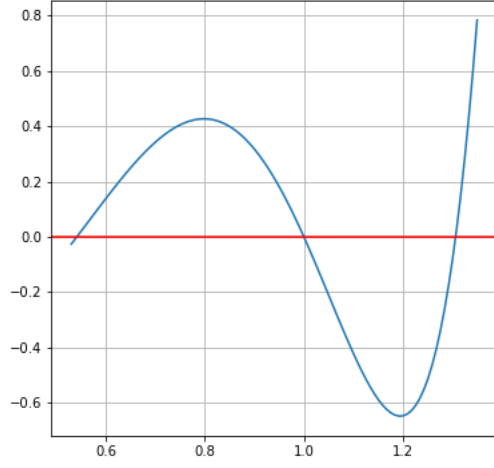
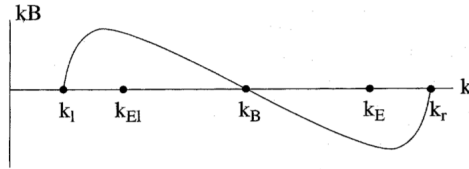Figure 2.1: Busse Balloon for Swift Hohenberg, $R = .5$

Fig. 2. Graph of kB versus k. $k_l(R), k_r(R)$ are the borders of the neutral stability curve. $\nabla \cdot kB$ is elliptic negative in $k_B < k < k_E$, hyperbolic in $k_{El} < k < k_B$ and $k_E < k < k_r$, elliptic positive in $k_l < R < k_{El}$. $k_{El}(R)$ and $k_E(R)$ are the left and right Eckhaus instability boundaries. k_B is the zig-zag instability boundary. The region in (R, k) space for which $k_B(R) \le k < k_E(R)$ is called the Busse balloon. k_{El} and k_E are the wavenumbers when kB is maximum and minimum respectively.

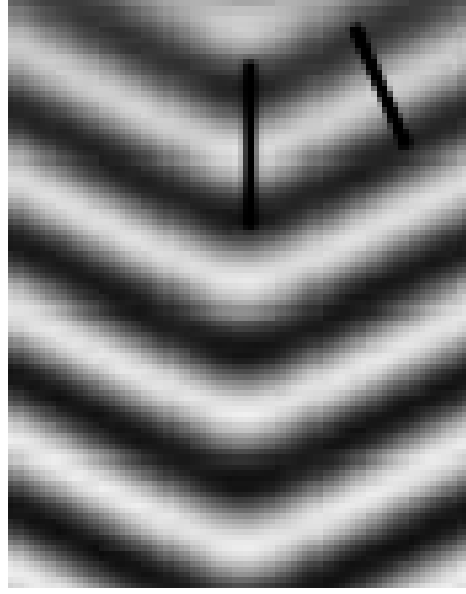Figure 2.2: Generic Busse Balloon

7

Figure 2.3: Change in wavelength along line defects

limited range of wave numbers where these values are satisfied. This range of wave numbers is knowen as the Busse-Balloon, and is the range $k_B < k < k_E$ as labeled in figure 2.2. It turns out for natural patterns, almost everywhere $k = k_B$, however along line defects we will have $k < k_B$.

Consider, for example, the scenario depicted in figure 2.3. We see that along the line defect, the pattern has a longer wavelength. This means that the local spatial frequences are smaller than they are along most of the pattern, where the wavenumber is close to k_B. Thus, along the line defect $k < K_B$, which lies outside of the Busse Balloon. Hence, the unregularized Cross-Newell phase diffusion equation is ill-posed along line defects, and regularization is required.

To regularize the Cross-Newell phase diffusion equation, we analyze the $\mathcal{O}(\epsilon^2)$ part of the energy, $\overline{E_2}$. We have that

$$\overline{E_2} = \int \left((2\boldsymbol{k} \cdot \nabla A + \nabla \cdot \boldsymbol{k}A)^2 + 2(1 - k^2)A\nabla^2 A \right) d\boldsymbol{x}. \tag{2.27}$$

It turns out that since $\nabla_{\boldsymbol{x}} = \boldsymbol{k}\frac{\partial}{\partial \theta} + \epsilon\nabla_{\boldsymbol{X}}$, the terms either involve differentiating $\boldsymbol{k}$ as it changes direction along the phase contour, or differentiation of k^2 in the direction of $\boldsymbol{k}$. The terms $2\boldsymbol{k} \cdot \nabla A$ and $A\nabla^2 A$ are small, and $\overline{E_2}$ can be well approximated by

$$\int A^2(k_B^2)(\nabla \cdot \boldsymbol{k})^2 d\boldsymbol{x}. \tag{2.28}$$

Computing its variation, we obtain the regularized Cross-Newell phase diffusion equation

$$A^2(k_B^2)\Theta_T + \nabla \cdot \boldsymbol{k}B + \epsilon^2 A^2(k_B^2)\nabla^4\Theta = 0. \tag{2.29}$$

Moreover, we can approximate the energy $\overline{E}$ by

$$\overline{E} = \int \left(\left(\left(\frac{d}{dk^2} B(k^2) \right) \right)_{k_B^2} (k^2 - k_B^2) + \epsilon^2 (\nabla \cdot \boldsymbol{k})^2 A^2(k_B^2) \right) d\boldsymbol{x}. \tag{2.30}$$

The $\mathcal{O}(\epsilon^0)$ contribution is the "strain" energy, and the $\mathcal{O}(\epsilon^2)$ contribution is the "bending" energy.

3 The regularized phase diffusion equation for real fields

In the case of real fields, the Swift-Hohenberg equation has microscopic energy functional

$$E = \int \left(((\nabla^2 + 1)w)^2 - \frac{1}{2} R w^2 + \frac{1}{4} w^4 \right) d\boldsymbol{x}. \tag{3.1}$$

In this case, the microscopic equation is

$$w_t = -\frac{\delta E}{\delta w} = -(\nabla^2 + 1)^2 w + Rw - w^3. \tag{3.2}$$

Note that equation (3.2) admits stationary solutions for striped patterns

$$w(\boldsymbol{x}, t) = w(\theta; \{A_n(k^2)\}, R) = \sum A_n(k^2) \cos(n\theta). \tag{3.3}$$

In the real field case, our modulation ansatz is given by (1.1),

$$w(\boldsymbol{x}, t) = w(\theta; \{A_n(k^2)\}, R; \nabla\theta = \boldsymbol{k}(\boldsymbol{X}, T) = \nabla_{\boldsymbol{X}}\Theta(\boldsymbol{X}, t)). \tag{3.4}$$

The procedure to derive the phase diffusion equation is the same as it was for the case of complex fields. However, the energy is not automatically averaged, making the procedure far more delicate. We simply state the key results.

The microscopic equations evolve according to

$$w_t \delta w = -\delta E. \tag{3.5}$$

Upon averaging over θ, one obtains

$$\langle w_\theta^2 \rangle \theta_t \delta\theta = -\delta\overline{E} \tag{3.6}$$

The averaged energy to leading order is given by

$$\overline{E_0} = \left(-\frac{1}{4} \langle w^4 \rangle + K \right) dxdy \tag{3.7}$$

Again, k_B^2 is defined so as to satisfy

$$\frac{d}{dk^2} \left(\frac{1}{4} \langle w^4 \rangle \right) = 0, \tag{3.8}$$

9

and defining K as we did for the complex case, obtain

$$\overline{E_0} = \int \left(\frac{1}{4} \langle w^4 \rangle \right)_{k^2}^{k_B^2} dx dy. \tag{3.9}$$

Considering just the leading order contribution of the energy, we can obtain the unregularized diffusion equation by taking the variaton of $\overline{E_0}$, and obtain

$$\langle w_\theta^2 \rangle \Theta_T + \nabla_{\boldsymbol{X}} \boldsymbol{k} B(k^2) = 0, \tag{3.10}$$

where

$$B(k^2) = 2 \frac{dE_0}{dk^2}, \tag{3.11}$$

where E_0 here is used to denote the integrand of $\overline{E_0}$. Note that in the complex case, we had $B(k^2) = \frac{dE_0}{dk^2}$.

The fact that the $\mathcal{O}(\epsilon)$ terms vanish in the averaged energy is not as clear in the case of the real field, but it still holds. The argument as to why is omitted for the time being.

Considering the $\mathcal{O}(\epsilon^2)$ terms, we argue in a similar fashion as we did for the case of complex fields. All terms involving $(\boldsymbol{k} \cdot \nabla_{\boldsymbol{X}})$ acting on the amplitudes yield terms proportional to $\frac{dA_n(k^2)}{dk^2}(\boldsymbol{k} \cdot \nabla_{\boldsymbol{X}} k^2)$ which can be written as $\boldsymbol{k} \cdot \nabla_{\boldsymbol{X}}(k^2 - k_B^2)$. Since $k^2 - k_B^2$ is small almost everywhere, there terms are negligible compared to the terms proportional to $\nabla \cdot \boldsymbol{k}$. Via integration by parts, one can obtain

$$\epsilon^2 \int \langle w_\theta^2 \rangle (\nabla \cdot \boldsymbol{k})^2 d\boldsymbol{x} \approx \epsilon^2 \langle w_\theta^2 \rangle_{k_B} \int (\nabla \cdot \boldsymbol{k})^2 d\boldsymbol{x}. \tag{3.12}$$

The regularized phase diffusion equation is then

$$\langle w_\theta^2 \rangle \Theta_T + \nabla \cdot \boldsymbol{k} B + \epsilon^2 \langle w_\theta^2 \rangle \nabla^4 \Theta = 0. \tag{3.13}$$

As we did for the complex field case, we can write the phase diffusion equation as a gradient flow, with the form

$$\eta \nabla^4 \theta + \nabla \cdot \boldsymbol{k} B = -\frac{\delta \overline{E}}{\delta \theta} \tag{3.14}$$

$$\overline{E} = \int \left(\frac{1}{2} \eta |\nabla^2 \theta|^2 + \frac{\alpha}{2} G^2 \right) d\boldsymbol{x} \tag{3.15}$$

$$G^2 = -\frac{1}{\alpha} \int_{k_B^2}^{k^2} B dk^2 \tag{3.16}$$

$$\alpha = -\frac{1}{4k_B} |B'(k_B)|. \tag{3.17}$$

In this form, the first term measures the "bending" energy, whereas the second term measures the "stretching" energy.

As a quick demonstration of the fact that the wavenumber is almost constant throughout the pattern, and that the solution evolves so as to minimize an energy, figure 3.1 shows a solution of Swift-Hohenberg on the square alongside its energy density, and keep track of the total energy. We see that the energy tends to condense around bends within the pattern. We use random initial conditions for this solution.

Total energy corresponding to figure 3.1

```
total energy at time 15:   -33.888597248321645
total energy at time 20:   -52.26404570245001
total energy at time 25:   -77.2887255255116
total energy at time 30:   -109.74938099881015
total energy at time 199:   -338.9569147336093
total energy at time 200:   -338.9892785820569
```
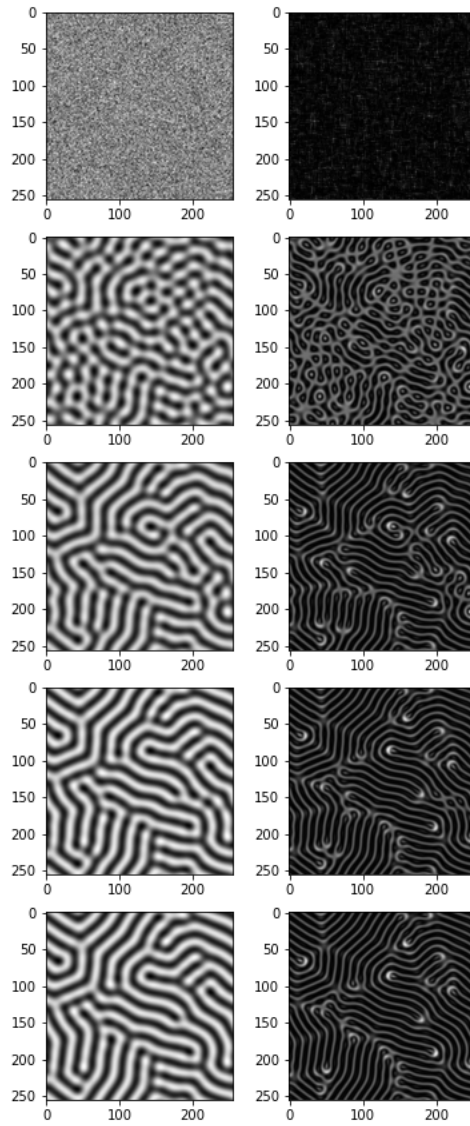
Figure 3.1: Swift-Hohenberg solution on the square, $R = .5$

4 Self-Dual Solutions and an Open Challenge

We are interested in stationary solutions of the RCN, namely solutions of

$$\eta\nabla^4\theta + \nabla \cdot \boldsymbol{k}B = -\frac{\delta\overline{E}}{\delta\theta} = 0. \tag{4.1}$$

Many stationary solutions can be deduced by balancing the strain and bending energies of $\overline{E}$. To name a few, the creation of VX pairs (figure 4.1), and concave and convex disclinations (figure 4.2).

There is a particular scenario that can be observed experimentally and in numerical simulations that is not yet deduced from the RCN. Numerically, this can be depicted by solving Swift-Hohenberg on an ellipse, using the Eikonal Solution as an initial condition. What one observes qualitatively is that the eikonal solution generates pointy edges where the stripes meet along the major axis of the ellipse. These points rapidly transition into a nipple instability, at which point a new state emerges. This state appears like a set of stair steps for stripes close to the major axis. An explanation for how this state emerges, in terms of the self-dual solution, is unclear. Figure 4.3 demonstrates solutions having this behavior, with their associated energy density.

Total energy corresponding to figure 4.3

```
total energy at time 15:   -167.19072805295662
total energy at time 20:   -261.4739829791277
total energy at time 25:   -391.7822674764031
total energy at time 30:   -560.5206723618704
total energy at time 199:  -1518.3264485682134
total energy at time 200:  -1518.3769630101526
```
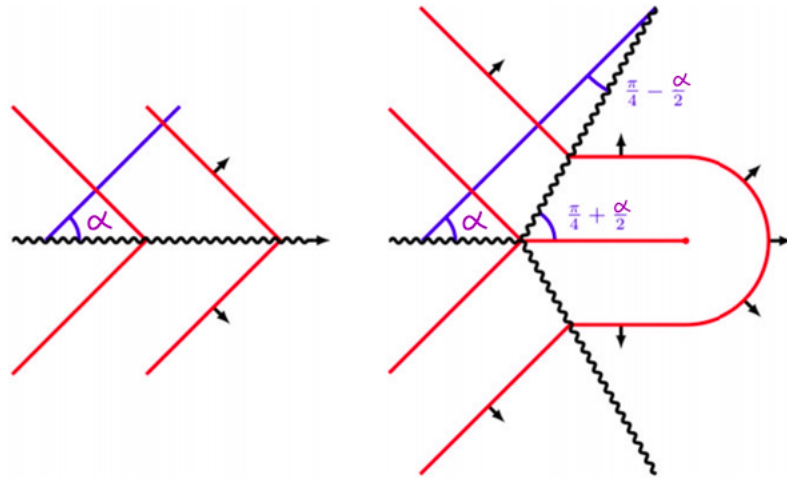
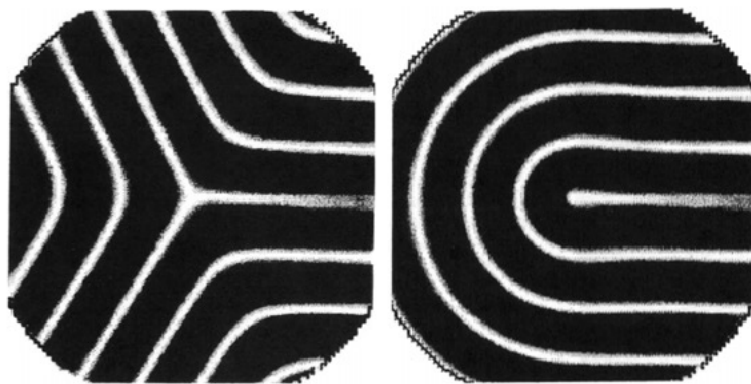Figure 4.1: The nipple instability and birth of VX pair

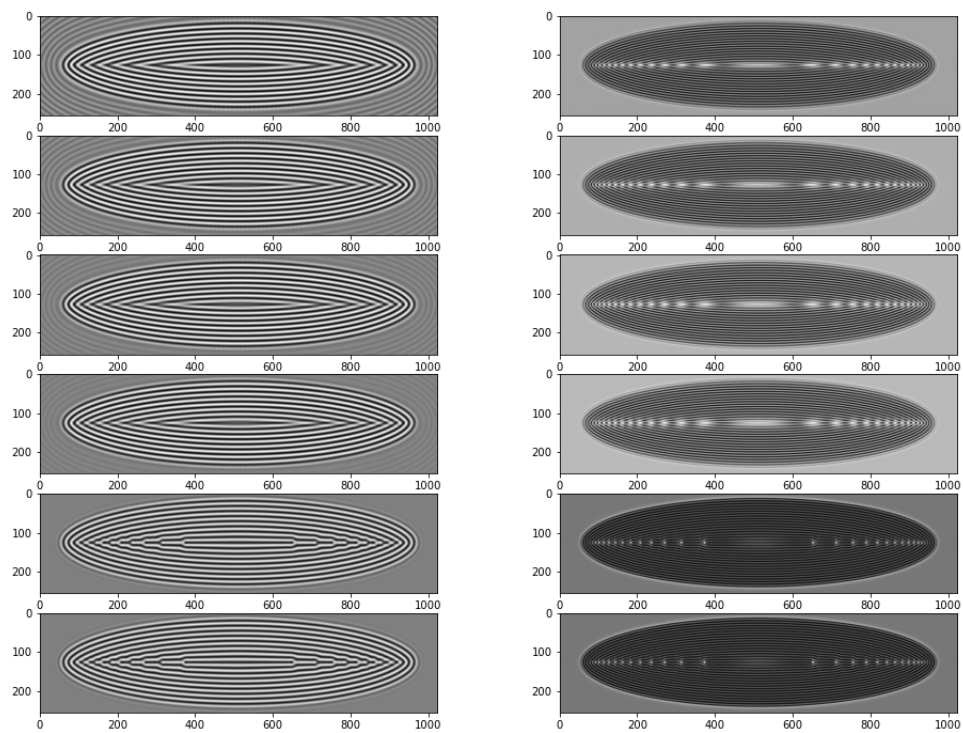Figure 4.2: A concave and convex disclination

Figure 4.3: Swift Hohenberg solution on an ellipse, with eikonal initial condition

5 Machine Learning Experiments

5.1 SINDy-like methods for PDEs

Note that the problem at hand involves a microscopic model exhibiting behavior that is not yet deduced from the macroscopic model. This raises the possibility that the macroscopic model does not capture all aspects of the microscopic equations. Thus, one may be tempted to find an additional term to the macroscopic model.